plates are specialized for rapid long bone growth. Mammalian growth plates are capable of rapid bone elongation, in large part through longitudinally directed cellular swelling of the hypertrophic chondrocytes (*19*), whereas an increased population of proliferative chondrocytes appears to be significant in birds (*15*). Cellular swelling through water uptake allows great increase in cell volume without excessive energy expenditure. The avian plan of increased proliferation is energy demanding, but may be compensated by the coadaptation of reduced bone production. Although convergent evolution of rapid determinate growth in mammals and birds has been achieved by different cellular mechanisms, a high metabolic rate is required in both, and this energy-demanding adaptation seems to have been present in dinosaurs.

REFERENCES AND NOTES

1. D. S. Howell and D. D. Dean, in *Disorders of Bone and Mineral Metabolism*, F. L. Coe and M. J. Favus, Eds. (Raven, New York, 1992), pp. 313–353.
2. G. J. Breur *et al.*, *J. Orthop. Res.* **9**, 348 (1991); E. B. Hunziker *et al.*, *J. Bone Jt. Surg. Am. Vol.* **69**, 162 (1987); N. F. Kember and J. K. Kirkwood, in *Fundamentals of Bone Growth: Methodology and Applications*, A. D. Dixon, B. G. Sarnat, D. A. N. Hoyte, Eds. (CRC Press, Boca Raton, FL, 1991), pp. 153–162; J. L. Kuhn, J. D. Hornovich, E. E. Lee, *Transactions of the 39th Annual Meeting of the Orthopaedic Research Society* **18**, 695 (1993).
3. J. R. Horner, *J. Vertebr. Paleontol.* **3**, 29 (1983).
4. Phylogenetic classification of living amniotes (including birds, lizards, and mammals) into reptilian groups reflects hypotheses concerning recency of origination from common ancestors. The placement of animals into groups by systematists is based on analysis of the distribution of advanced (derived) character states that evolve in a species and are then passed on to its descendants. W. Hennig, *Phylogenetic Systematics* (Univ. of Illinois Press, Urbana, 1966); P. C. Sereno, in *Dinosaur Systematics*, K. Carpenter and P. J. Currie, Eds. (Cambridge Univ. Press, Cambridge, 1990), pp. 9–20.
5. J. C. Lorenz and W. Gavin, *Mont. Geol. Soc. Annu. Field Conf. Guideb.* 175 (1984).
6. J. R. Horner, *Nature* **297**, 675 (1982).
7. ——, *Sci. Am.* **250**, 130 (April 1984); —— and R. Makela, *Nature* **282**, 296 (1979).
8. Calcite crystals fill the interstices of the dinosaur bone, preventing microscopic viewing. Calcite was etched with 10% acetic acid without altering the ultrastructure of the dinosaur bone (C. Barreto and R. M. Albrecht, *Scanning Microsc.*, in press). The bone appears to have not been replaced by minerals from the ground water during >70 million years of burial, as the elemental composition is consistent with that of modern bone and unlike that of the calcite deposited in the bone interstices.
9. A. Boyde and S. J. Jones, in *Cartilage: Structure, Function, and Biochemistry*, B. K. Hall, Ed. (Academic Press, London, 1983), vol. 1, pp. 105–148.
10. Mean Ca:P atomic percent ratios were chicken, 1.5578 and *Maiasaura*, 1.5591. These values are compatible with those for hydroxyapatite. Electron probe analysis was conducted at 15 to 20 kV at a take-off angle of 35° on a JSM 35-C JEOL scanning electron microscope equipped with a Tracor Northern TN-5500 EDX.
11. J. Gauthier, in *The Origin of Birds and the Evolution of Flight*, K. Padian, Ed. (Academic Press, San Francisco, 1986), pp. 1–55.
12. J. H. Ostrom, in *A Cold Look at the Warm-Blooded Dinosaurs*, R. D. K. Thomas and E. C. Olson, Eds. (Westview, Boulder, CO, 1980), pp. 15–54.
13. K. Padian, in *Third North American Paleontological Convention Proceedings*, B. Mamet and M. J. Copeland, Eds. (Business and Economic Service, Ltd., Toronto, 1982), vol. 2, pp. 387–392; R. A. Thulborn, in *Hornibrook Symposium*, R. Cooper, Ed. (New Zealand Geological Society, Lower Hutt, 1985), pp. 90–92.
14. R. T. Bakker and P. M. Galton, *Nature* **248**, 168 (1974); M. J. Benton, in *The Dinosauria*, D. B. Weishampel, P. Dodson, H. Osmolska, Eds. (Univ. of California Press, Berkeley, 1990), pp. 11–30; J. F. Bonaparte, *J. Paleontol.* **50**, 808 (1976); F. E. Novas, *ibid.* **63**, 677 (1989); *Palaeontology* **35**, 51 (1992); P. C. Sereno *et al.*, *Nature* **361**, 64 (1993); P. C. Sereno and F. E. Novas, *Science* **258**, 1137 (1992).
15. C. Barreto and N. J. Wilsman, *Res. Vet. Sci.*, in press.
16. J. K. Kirkwood, N. F. Kember, D. J. Spratt, *Proceedings of the First International Conference on Zoological and Avian Medicine*, Oahu, HI (American Association of Zoological Veterinarians, Philadelphia, PA, 1987).
17. A. Chinsamy, *Palaeontol. Afr.* **27**, 77 (1990); D. J. Varricchio, *J. Vertebr. Paleontol.* **13**, 99 (1993).
18. R. T. Bakker, *Nature* **238**, 81 (1972); M. Bouvier, *Evolution* **31**, 449 (1977); J. D. Currey, *Paleontology* **5**, 238 (1962); R. E. H. Reid, *Nature* **292**, 49 (1981); *Geol. Mag.* **120**, 191 (1983); *ibid.* **121**, 589 (1984); *Mod. Geol.* **11**, 133 (1987); A. J. de Ricqles, *Evol. Theory* **1**, 51 (1974); in *Morphology and Biology of Reptiles*, A. d'A. Bellairs and C. Cox, Eds. (Linnean Society, London, 1976), pp. 123–150; in (*12*), pp. 103–139.
19. J. A. Buckwalter and R. D. Sjolund, *Iowa Orthop. J.* **9**, 25 (1990).

20. We thank M. Kohler and T. Kohler for their support, D. L. Clark and L. R. Stanford for comments on the manuscript, and R. Noll of the Department of Materials Science and Engineering for use of that facility. Supported by the Windway Foundation, Incorporated.

23 August 1993; accepted 29 October 1993

Mantle Plume Helium in Submarine Basalts from the Galápagos Platform

D. W. Graham, D. M. Christie, K. S. Harpp, J. E. Lupton

Helium-3/helium-4 ratios in submarine basalt glasses from the Galápagos Archipelago range up to 23 times the atmospheric ratio in the west and southwest. These results indicate the presence of a relatively undegassed mantle plume at the Galápagos hot spot and place Galápagos alongside Hawaii, Iceland, and Samoa as the only localities known to have such high helium-3/helium-4 ratios. Lower ratios across the rest of the Galápagos Archipelago reflect systematic variations in the degree of dilution of the plume by entrainment of depleted material from the asthenosphere. These spatial variations reveal the dynamics of the underlying mantle plume and its interaction with the nearby Galápagos Spreading Center.

Isotope and trace element studies have indicated the scale of mantle heterogeneity beneath ocean islands and have shown that different mantle regions are sampled by hot spot volcanism as the degree of partial melting and depth of melt extraction vary through time (*1*). Spatial variability can also be characterized by the study of lavas of similar age from different volcanoes that are simultaneously active in the same region. The Galápagos Archipelago, where coeval volcanism has occurred over distances of ~500 km, is an exceptional locality for such studies (*2*). The Sr-Nd-Pb isotopic variations in Galápagos lavas have been interpreted to indicate that asthenospheric mantle has been variably entrained into an upwelling mantle plume (*2, 3*). As the thermally buoyant plume rises, it bends from shear flow in the upper mantle as a result of overlying plate motion, and surrounding mantle material is entrained as its viscosity decreases because of heating by the plume (*4*). In addition, hot spot ridge interaction has produced elevated La/Sm and $^{87}Sr/^{86}Sr$ ratios along the Galápagos Spreading Center to the north (*5*). However, He isotope ratios along the ridge are similar to those of normal mid-ocean ridge basalts (MORBs) (*6*), suggesting that the hot spot component reaching the ridge does not have a high $^{3}He/^{4}He$ ratio (*7*). In this report, we present and discuss new He isotope results for submarine basalt glasses from the Galápagos platform. The observed He isotope variations are sensitive to mixing between magmas or their mantle sources, to gas loss, and to crustal assimilation, providing additional insight as to the origin of the plume and its interaction with the shallow mantle and nearby spreading center.

We measured $^{3}He/^{4}He$ ratios as well as He and Ne concentrations in a suite of basalt glasses from seamounts around the Galápagos platform and in olivine phenocrysts from four subaerial samples (Fig. 1 and Table 1). Two subaerial samples are from Isla Floreana, and these have the most radiogenic Sr and Pb isotope compositions

D. W. Graham and D. M. Christie, College of Oceanic and Atmospheric Sciences, Oregon State University, Corvallis, OR 97331.
K. S. Harpp, Department of Geological Sciences, Cornell University, Ithaca, NY 14853.
J. E. Lupton, National Oceanic and Atmospheric Administration, Pacific Marine Environmental Laboratory, Hatfield Marine Science Center, Newport, OR 97365.

measured in the Galápagos (2); the other two are from Isla Santa Fe. Analyses were performed by crushing in vacuum, thereby liberating gases trapped in vesicles and fluid inclusions (8).

Lavas with high $^3He/^4He$ ratios are found in the western and southern parts of the archipelago (Fig. 1). The highest $^3He/^4He$ ratio, 22.8 R_A, is from a transitional basalt glass (sample RC01) from a volcanic ridge that appears to be the submarine extension of a northwest-trending radial fissure zone on Fernandina (9). The location of this sample is consistent with the standard hot spot model, in which lavas from the leading western edge of the Galápagos platform contain relatively undiluted plume He as the Nazca plate moves east-southeast over a fixed plume source. Several samples from the southwestern margin of the Galápagos platform also have high $^3He/^4He$ ratios. Values between 16.5 and 18.7 R_A occur along the southern escarpment of the platform between Isabela and Floreana, and a value of 14.5 R_A was measured for olivine separated from a cumulate wehrlite xenolith from the main volcanic series of Isla Floreana (Fig. 1). One important exception to this pattern is that alkali basalt glasses from dredge 25, located on the western flank of Fernandina and close to sample RC01, have low and variable $^3He/^4He$ ratios (1.8 to 7.0 R_A), generally accompanied by low He concentrations (Table 1). These low $^3He/^4He$ ratios and He concentrations are comparable to those for young alkali basalt glasses from seamounts near the East Pacific Rise (*10*) and for intermediate and acidic rocks from Iceland (*11*). The He isotope signatures of these magmas have probably been modified by magmatic degassing and crustal assimilation associated with a prolonged residence in subvolcanic magma chambers (*11*).

Seamounts from the northeastern part of the platform (dredges 9 to 14) have $^3He/^4He$ ratios between 7.3 and 8.5 R_A (Fig. 1), typical of the depleted mantle source for MORB. Samples from Isla Santa Fe near the center of the archipelago have similar or slightly higher values, with a maximum of 9.5 R_A. Along the Wolf-Darwin lineament (dredges 26 to 30), values range from 6.9 to 8.8 R_A. Thus, the He isotope data can be divided into three regional groups: the western and southern margins, the northeastern seamounts, and the Wolf-Darwin lineament. Consistent with results from other geochemical systems (2), no systematic variations with time are apparent because ages of the three regions overlap (*12*).

Geographic variations in Sr, Nd, and Pb isotope ratios across the Galápagos platform show that values similar to those found in MORBs occur close to the archipelago center, flanked by more enriched values to the north, west, and south (*2, 3*). This pattern has been thought to reflect the entrainment of asthenosphere into a plume that is being sheared by upper mantle convective flow (*2, 4*). In general, the spatial variation in $^3He/^4He$ ratios is consistent with this model, as well as with the plume having a high $^3He/^4He$ ratio. However, there are two additional complexities. First, there is a north-south heterogeneity in Sr, Nd, and Pb isotope compositions across the plume. Lavas from Pinta and Floreana are derived from similar, but distinct, enriched sources (*2*). This heterogeneity introduces some uncertainty when the He isotope results are related to the other isotopic systems. We do not have He analyses for lavas from the island of Pinta because of a lack of samples with sufficient olivine, and the question of whether Pinta has high $^3He/^4He$ ratios will need to be answered to evaluate fully the degree of He isotope heterogeneity within the plume. Second, the He results for the Wolf-Darwin lineament do not fit the isotopic pattern observed across the archipelago in a simple way (Fig. 1).

The Wolf-Darwin lineament is a line of seamounts and islands extending northwestward from the platform to the Galápagos Spreading Center and may have formed

Table 1. He isotopes in Galápagos basalts. Submarine samples were recovered by the Plume 2 expedition aboard the research vessel *Thomas Washington* in 1990. Sample designations are dredge number and sample number. Rock types are th, tholeiite; tr, transitional basalt; and ab, alkali basalt, according to (*30*); x, wehrlite xenolith in alkali olivine basalt flow. Samples were hand-picked glasses except where noted otherwise (ol, olivine and cpx, clinopyroxene). FL-3 ol + cpx are aggregates of olivine and clinopyroxene, typically >5 mm in size. This xenolith sample is from the main lava series, and the Sr, Nd, and Pb isotope values measured for the xenolith (*2*) have been used for plotting purposes in Figs. 2 and 3. Gas extractions were performed by in vacuo crushing. Uncertainties in the $^3He/^4He$ ratio are the quadrature sum of in-run statistical errors plus uncertainties in air standard and blank analyses. He/Ne ratios were measured but are not reported here. Low He/Ne ratios can be used as an indicator of possible air contamination. Corrections to the $^3He/^4He$ ratio after this procedure are comparable to the reported uncertainties for all samples except 25-1 and 25-4; for FL-3 ol + cpx, the corrected value agrees with the slightly higher $^3He/^4He$ values measured for olivine separates alone from this sample.

Sample	Latitude	Longitude (°W)	Depth (m)	Rock type	$^3He/^4He$ (R/R_A)	[He] (10^{-6} cm^3/g at STP)
South and west region						
PL2 RC 01	0° 13.9′S	91° 45.3′	1840	tr	22.80 ± 0.15	1.05
Replicate	0° 13.9′S	91° 45.3′	1840	tr	22.87 ± 0.15	0.936
PL2 23-1 ol	1° 20.0′S	90° 59.8′	3400	tr	18.70 ± 0.24	0.0286
PL2 24-14	1° 17.5′S	90° 54.9′	2700	tr	16.84 ± 0.11	0.0631
PL2 24-32	1° 17.5′S	90° 54.9′	2700	tr	16.56 ± 0.19	0.0114
PL2 24-32 ol	1° 17.5′S	90° 54.9′	2700	tr	14.67 ± 0.60	0.0046
PL2 24-37	1° 17.5′S	90° 54.9′	2700	tr	17.21 ± 0.13	0.0836
PL2 25-1	0° 16.3′S	91° 46.9′	2200	ab	4.75 ± 0.10	0.0156
PL2 25-3	0° 16.3′S	91° 46.9′	2200	ab	6.97 ± 0.39	0.0029
PL2 25-4	0° 16.3′S	91° 46.9′	2200	ab	1.94 ± 0.15	0.0058
Replicate	0° 16.3′S	91° 46.9′	2200	ab	1.80 ± 0.12	0.0079
Northeast region						
PL2 9-29	0° 28.1′S	88° 32.0′	1300	th	8.19 ± 0.05	3.29
PL2 10-8	0° 33.0′S	88° 32.0′	1300	th	7.72 ± 0.42	0.007
PL2 12-1	0° 12.8′S	88° 39.2′	1200	th	8.04 ± 0.07	0.144
PL2 13-25	0° 4.6′N	89° 2.7′	1000	th	7.27 ± 0.04	1.25
PL2 14-8	0° 4.1′N	89° 7.1′	1500	th	8.78 ± 0.05	0.831
Wolf-Darwin lineament						
PL2 26-7	0° 50.0′N	91° 17.5′	600	tr	8.81 ± 0.05	6.81
PL2 26-16	0° 50.0′N	91° 17.5′	600	tr	8.79 ± 0.05	5.59
PL2 26-21	0° 50.0′N	91° 17.5′	600	tr	8.80 ± 0.05	5.09
PL2 26-25	0° 50.0′N	91° 17.5′	600	tr	8.51 ± 0.05	17.6
PL2 27-1	0° 52.8′N	91° 19.6′	1500	tr	8.51 ± 0.05	10.1
PL2 27-17	0° 52.8′N	91° 19.6′	1500	—	8.53 ± 0.05	6.87
PL2 28-1	1° 1.5′N	91° 33.3′	1200	tr	8.42 ± 0.05	5.31
PL2 28-11	1° 1.5′N	91° 33.3′	1200	tr	8.45 ± 0.05	8.72
PL2 29-2	1° 54.0′N	92° 9.7′	1750	th	7.88 ± 0.05	0.734
PL2 29-3	1° 54.0′N	92° 9.7′	1750	th	7.81 ± 0.05	0.889
PL2 30-1	1° 35.5′N	91° 55.6′	2200	th	6.87 ± 0.08	0.989
Islands						
FL-3 ol	Floreana			x	14.54 ± 0.15	0.0668
FL-3 ol + cpx	Floreana			x	13.99 ± 0.20	0.0364
E-108 ol	Floreana			ab	7.74 ± 0.51	0.0152
SF-13 ol	Santa Fe			ab	8.18 ± 0.52	0.0252
G86-5 ol	Santa Fe			ab	9.52 ± 0.62	0.0092

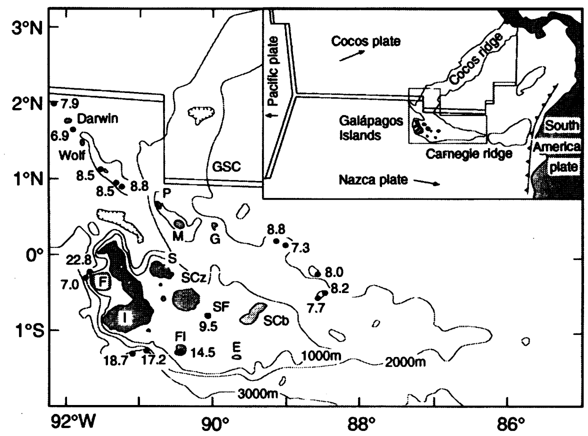

Fig. 1. Geographic variation of $^3He/^4He$ across the Galápagos platform. Numbers indicate the highest values from each island or dredge haul. GSC is the Galápagos Spreading Center. Island abbreviations: F, Fernandina; I, Isabela; Fl, Floreana; E, Española; SF, Santa Fe; SCz, Santa Cruz; S, Santiago; SCb, San Cristobal; G, Genovesa; M, Marchena; and P, Pinta.

by the channeled flow of the plume toward the ridge (*13*) or by the interaction of a lithospheric fault with the plume (*14*). Isotope compositions of samples from the Wolf-Darwin lineament and the northeastern seamounts indicate that the mantle beneath those regions contains a component with MORB isotope characteristics ($^3He/^4He$ = 8.5 R_A, $^{87}Sr/^{86}Sr$ < 0.7026, and $^{206}Pb/^{204}Pb$ < 18.4). Along the lineament, $^3He/^4He$ ratios are generally low, with the most radiogenic He and Sr values from a small seamount between Wolf and Darwin islands (Fig. 1), where $^3He/^4He$ is ~7 R_A and $^{87}Sr/^{86}Sr$ is ~0.7030. These values are similar to those found along the Galápagos Spreading Center near 92°W, where the lineament intersects the ridge axis (*5, 7*), and where the ridge has the highest $^{87}Sr/^{86}Sr$ and lowest $^{143}Nd/^{144}Nd$ because of the interaction with the hot spot (*5*). No high $^3He/^4He$ ratios are known along either the Wolf-Darwin lineament or the Galápagos Spreading Center. This absence suggests that the behavior of volatile and lithophile elements has been quite different during mantle upwelling, partial melting, or both. Helium concentrations vary over a large range along the Wolf-Darwin lineament, and lower $^3He/^4He$ ratios tend to correlate with lower He contents (Table 1). This trend suggests that the plume's high $^3He/^4He$ signature may have been diluted by degassing followed by either radiogenic ingrowth or crustal assimilation. A degassed magma with low He concentration is particularly susceptible to the lowering of its $^3He/^4He$ ratio by these processes (*15*). Of these alternatives, crustal assimilation seems less likely, because it would not strongly affect spreading center lavas and therefore cannot account for the absence of high $^3He/^4He$ ratios along the Galápagos Spreading Center. The absence of a high $^3He/^4He$ signature along both the Wolf-Darwin lineament and the Galápagos Spreading Center (*7*) is more likely due to the degassing of plume material at depth during lateral transport toward the ridge axis (*16*).

Relations between $^3He/^4He$ and the isotopes of Sr, Nd, and Pb for the data set as a whole are complex (Fig. 2), partly because of the presence of at least three mantle components in the Galápagos region (*2*). Lavas from the southern and western regions have the highest $^3He/^4He$ and most enriched Sr, Nd, and Pb isotope ratios. In detail, however, the highest $^3He/^4He$ ratios are associated with moderate Sr, Nd, and

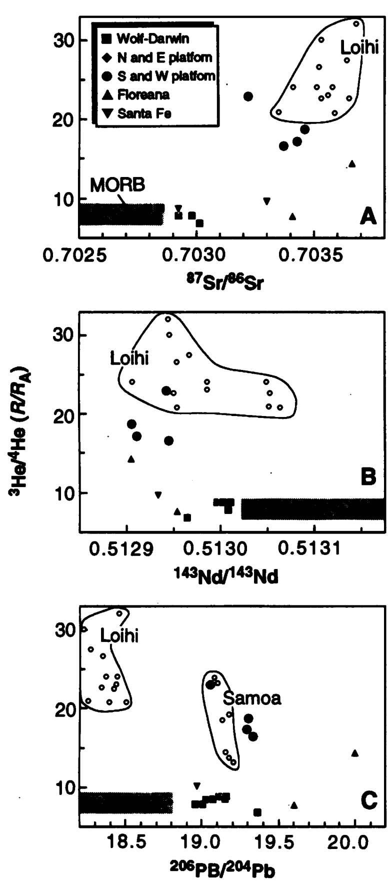

Fig. 2. Ratio of $^3He/^4He$ versus (**A**) $^{87}Sr/^{86}Sr$, (**B**) $^{143}Nd/^{144}Nd$, and (**C**) $^{206}Pb/^{204}Pb$. The Sr, Nd, and Pb data for Loihi seamount (*26*) and Pb data for Samoa (the Sr and Nd values at Samoa are well outside of the range shown) (*24*) are shown as small open circles. Shaded field shows the range of Pacific MORB isotopes (*28*) for comparison.

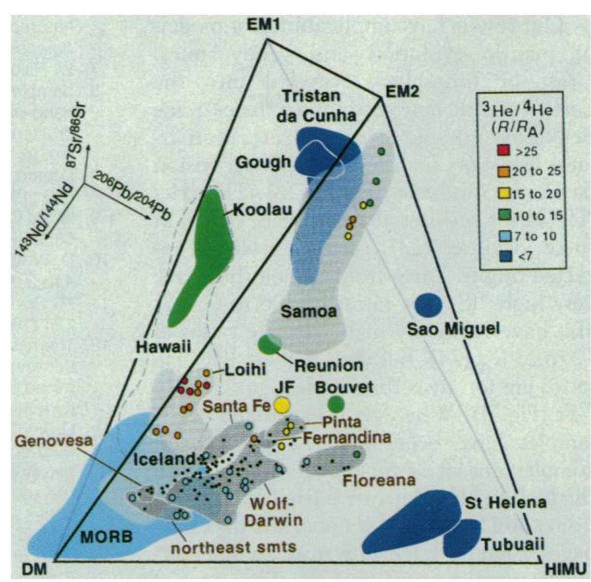

Fig. 3. An Sr-Nd-Pb isotopic tetrahedron encompassing the range for oceanic volcanic rocks (*21*). Abbreviations: DM, the depleted mantle source for MORB; HIMU, the high U/Pb component as discerned from radiogenic $^{206}Pb/^{204}Pb$ at the islands such as St. Helena; and EM1 and EM2, mantle components enriched in $^{87}Sr/^{86}Sr$. In this view, EM2 lies above the DM-EM1-HIMU plane, in which ~95% of the oceanic data lie (*21*). Insets show color coding for $^3He/^4He$ ratios and the relative orientation of the isotopic axes. The $^{87}Sr/^{86}Sr$ axis points out of the plane of the paper, and the origin for the relative isotopic scales occurs at the midrange of the oceanic data (near the lower right of the Samoa field). Samples analyzed for the full complement of Sr-Nd-Pb and He isotopes are shown as color-coded circles for Loihi seamount, Samoa (Tutuila), and the Galápagos samples analyzed in this study. Color fields represent islands where the same samples have not been analyzed for all the isotopes but where a multi-isotopic characterization can be made in a straightforward way on the basis of the range of measured values. Gray fields indicate localities where the highest $^3He/^4He$ ratios (>20 R_A) have been found (Loihi, Iceland, Samoa, and Galápagos). The field for Hawaii is transparent for clarity, except for Loihi seamount and the Koolau volcanic series of Oahu. JF, Juan Fernandez; smts, seamounts. Brown labels are for the Galápagos Archipelago. Small circles are Sr-Nd-Pb results (*2*) for Galápagos Island samples not yet analyzed for $^3He/^4He$. In general, the higher $^3He/^4He$ ratios are present toward the interior of the tetrahedron volume. He isotope data sources include (*8, 11, 23, 24, 26, 29*). The Sr-Nd-Pb data are from the literature.

Pb isotope ratios near Fernandina [$^{87}Sr/^{86}Sr \cong 0.7031$ to 0.7035, $\epsilon_{Nd} \cong 5$ to 6 (*17*), $^{206}Pb/^{204}Pb \cong 19.1$ to 19.4 (*2*)], while the most enriched Sr, Nd, and Pb isotope values are from Floreana, which has only a moderately high $^3He/^4He$ (14.5 R_A). The scatter in the relations between He isotopes and Sr, Nd, and Pb isotopes appears to reflect some heterogeneity within the plume, although it is unclear whether this is the same N-S heterogeneity recognized by White and co-workers (*2*). Lavas from the southern and western regions appear to represent mixtures between relatively undegassed mantle with a high $^3He/^4He$ ratio (which is strongest near Fernandina) and enriched, more degassed mantle. This enriched component is strongest along the southern part of the platform where the degree of partial melting is lower than in other regions of the Galápagos Archipelago (*2, 18*). It may represent recycled material incorporated into the plume, possibly at the core-mantle boundary (*19*), or as the plume passed through the transition zone at the base of the upper mantle (*20*). This explanation associates the relatively high ^3He component and moderate Sr, Nd, and Pb isotope compositions with the plume source itself. A second explanation attributes the enriched Sr-Nd-Pb isotope composition to the Galápagos plume source. This relation would mean that mantle material with high $^3He/^4He$ was entrained, perhaps from the deep mantle, into a plume whose ultimate source was recycled material (*21*).

Our results have implications for models of mantle evolution and geodynamics. Crust or lithosphere recycled into the Earth's mantle may account for the extreme Sr-Nd-Pb isotopic signatures at ocean island hot spots such as St. Helena, Tristan da Cunha, and São Miguel (*22*). The $^3He/^4He$ ratios are less than MORB values at these localities (*23*), consistent with a recycled origin. Lavas from Samoa that have very high $^{87}Sr/^{86}Sr$ ratios (0.706 to 0.707) also have relatively high $^3He/^4He$ ratios of 12 to 23 R_A (*24*), but their highest $^3He/^4He$ ratios are for lavas that are less enriched in ^{87}Sr (Fig. 3). Wherever ocean island basalt samples have been analyzed for the full complement of isotopes, those lavas with the highest $^3He/^4He$ ratios (that is, >20 R_A from Loihi Seamount, Samoa, and the Galápagos Islands) have only intermediate Sr-Nd-Pb isotope ratios (Fig. 3). Therefore, if a common reservoir with high $^3He/^4He$ is involved in hot-spot volcanism it must have intermediate Sr-Nd-Pb isotope compositions (*24–26*). The observation in the Galápagos, as well as at other islands, that lavas with high $^3He/^4He$ ratios have a range of Sr-Nd-Pb isotope ratios that are not typical of presumed mantle end members means that the ultimate source reservoir for ^3He is different from that for the other isotopic tracers. For example, the high $^3He/^4He$ reservoir may be the deep mantle or the core-mantle boundary, whereas the extreme Sr, Nd, and Pb isotope compositions may originate from recycled crust or lithosphere. The high $^3He/^4He$ reservoir may also be variably degassed (*27*) and contaminated with recycled materials. The different relations between $^3He/^4He$ and the isotopes of Sr, Nd, and Pb at ocean islands, such as in Fig. 3, reflect the age and type of recycled material present and the extent to which a mantle plume samples recycled material, the depleted upper mantle, and the high $^3He/^4He$ reservoir.

REFERENCES AND NOTES

1. M. D. Feigenson and F. J. Spera, *Geology* **9**, 531 (1981); C.-Y. Chen and F. A. Frey, *J. Geophys. Res.* **90**, 8743 (1985).
2. W. M. White, A. R. McBirney, A. R. Duncan, *J. Geophys. Res.* **98**, 19533 (1993).
3. D. J. Geist, W. M. White, A. R. McBirney, *Nature* **333**, 657 (1988); K. S. Harpp and W. M. White, *Eos* **71**, 1695 (1990).
4. M. A. Richards and R. W. Griffiths, *Nature* **342**, 900 (1989).
5. J.-G. Schilling, R. H. Kingsley, J. D. Devine, *J. Geophys. Res.* **87**, 5593 (1982); S. P. Verma and J.-G. Schilling, *ibid.*, p. 10838; ——, D. G. Waggoner, *Nature* **306**, 654 (1983).
6. Mid-ocean ridge basalts erupted away from hot spots have a range of $^3He/^4He$ ratios between 7 and 9 R_A, where R_A is the atmospheric ratio of 1.39×10^{-6}. Much higher $^3He/^4He$ ratios at some ocean island hot spots indicate the presence within the Earth of an additional reservoir with a lower time-integrated (U + Th)/^3He ratio. This reservoir is generally regarded to be less degassed than the MORB source, although this idea has recently been challenged [D. L. Anderson, *Science* **261**, 170 (1993)].
7. W. Rison and H. Craig, *Eos* **65**, 1139 (1984).
8. Samples weighing between 100 and 750 mg were hand-picked to be free of surficial contamination or alteration and prepared and analyzed according to established procedures [D. Graham, J. Lupton, F. Albarède, M. Condomines, *Nature* **347**, 545 (1990)].
9. W. W. Chadwick and K. A. Howard, *Bull. Volcanol.* **53**, 259 (1991).
10. D. W. Graham *et al.*, *Contrib. Mineral. Petrol.* **99**, 446 (1988).
11. M. Condomines *et al.*, *Earth Planet. Sci. Lett.* **66**, 125 (1983).
12. The northeastern seamounts have ^{40}Ar-^{39}Ar ages between 3.2 and 5.7 million years (Ma), determined by the incremental heating of holocrystalline rock interiors [C. W. Sinton, thesis, Oregon State University, Corvallis (1992)]. This technique circumvents problems with inherited ^{40}Ar in the glassy portions of submarine lavas [G. B. Dalrymple and J. G. Moore, *Science* **161**, 1132 (1968)]. These ages are older than seamounts of the Wolf-Darwin lineament, which have whole-rock K-Ar ages of 0 to 1.6 Ma [C. W. Sinton, thesis, Oregon State University, Corvallis (1992)], and older than lavas from Wolf and Darwin islands [0.4 to 1.6 Ma (2)]. The submarine samples from the southern and western margins with high $^3He/^4He$ ratios are from young flows (<0.2 Ma), on the basis of their whole-rock K-Ar ages, whereas the subaerial samples are from older flows [0.35 Ma for E-108 from the flank series of Floreana to 1.52 Ma for FL-3 from the Floreana main series and 0.72 Ma for G86-5 to 2.50 Ma for SF-13 from Santa Fe (2)].
13. W. J. Morgan, *J. Geophys. Res.* **83**, 5355 (1978).
14. M. A. Feighner and M. A. Richards, *Eos.* **72**, 579 (1991).
15. We infer that the $^3He/^4He$ ratios in these samples have not been modified by post-eruptive radiogenic ingrowth. The He trapped in vesicles remains effectively isolated from the radiogenic component generated in the glass over time scales of 10^5 years or longer [D. W. Graham, W. J. Jenkins, M. D. Kurz, R. Batiza, *Nature* **326**, 384 (1987)]. The radiogenic He production rate is 2.1×10^{-7} cm^3 per gram at STP per part per million U per million years (for Th/U = 3). Uranium and thorium concentrations in the glass sample with the lowest $^3He/^4He$ ratio and [He] from the Wolf-Darwin lineament (sample 30-1, with 0.24 ppm U) can be estimated from the K_2O content (0.36% by weight) and the narrow range of Th/U (~3) and K/U (1.27×10^4) in basalts [K. P. Jochum, A. W. Hofmann, E. Ito, H. M. Seufert, W. M. White, *Nature* **306**, 431 (1983)]. Sample 30-1 has a measured age of 0.25 Ma (*14*). The amount of ^4He produced for this sample is $\sim 1.2 \times 10^{-8}$ cm^3 per gram at STP, which is only 12% of the measured vesicle [He]. Although this amount is significant, this example demonstrates that none of the Wolf-Darwin samples had high $^3He/^4He$ ratios at the time of eruption, because all the remaining samples have higher [He] and lower U and Th contents.
16. D. W. Graham *et al.*, *Earth Planet. Sci. Lett.* **110**, 133 (1992); R. J. Poreda, J.-G. Schilling, H. Craig, *ibid.* **119**, 319 (1993).
17. The value for $\epsilon_{Nd} \cong$

$$\left(\frac{^{143}Nd/^{144}Nd_{measured}}{^{143}Nd/^{144}Nd_{CHUR}} - 1 \right) \times 10^4$$

where $^{143}Nd/^{144}Nd_{CHUR}$ is the value for a chondritic uniform reservoir at present [D. J. DePaolo and G. J. Wasserburg, *Geophys. Res. Lett.* **3**, 249 (1976)].
18. D. J. Geist, *J. Volcanol. Geotherm. Res.* **52**, 65 (1992); C. S. Bow and D. J. Geist, *ibid.*, p. 83.
19. G. F. Davies, *Earth Planet. Sci. Lett.* **99**, 94 (1990).
20. C. J. Allègre and D. L. Turcotte, *Geophys. Res. Lett.* **12**, 207 (1985).
21. S. R. Hart *et al.*, *Science* **256**, 517 (1992).
22. R. L. Armstrong, *Philos. Trans. R. Soc. London Ser. A* **301**, 443 (1981); C. G. Chase, *Earth Planet. Sci. Lett.* **52**, 277 (1981); A. W. Hofmann and W. M. White, *ibid.* **57**, 421 (1982); D. McKenzie and R. K. O'Nions, *Nature* **301**, 229 (1983); W. M. White, *Geology* **13**, 115 (1985); A. Zindler and S. Hart, *Annu. Rev. Earth Planet. Sci.* **14**, 493 (1986).
23. M. D. Kurz, W. J. Jenkins, S. R. Hart, *Nature* **297**, 43 (1982); D. W. Graham, S. E. Humphris, W. J. Jenkins, M. D. Kurz, *Earth Planet. Sci. Lett.* **110**, 121 (1992); M. D. Kurz, D. P. Kammer, A. Gulessarian, R. B. Moore, *Eos* **71**, 657 (1990).
24. K. A. Farley, J. H. Natland, H. Craig, *Earth Planet. Sci. Lett.* **111**, 183 (1992).
25. K. A. Farley and H. Craig, *Science* **258**, 821 (1992); S. R. Hart *et al.*, *ibid.*, p. 821.
26. M. D. Kurz *et al.*, *Earth Planet. Sci. Lett.* **66**, 388 (1983); W. Rison and H. Craig, *ibid.*, p. 407; H. Staudigel *et al.*, *ibid.* **69**, 13 (1984).
27. R. J. Poreda and K. A. Farley, *ibid.* **113**, 129 (1992); K. A. Farley and R. J. Poreda, *ibid.* **114**, 325 (1993).
28. W. M. White, A. W. Hofmann, H. Puchelt, *J. Geophys. Res.* **92**, 4881 (1987).
29. K. A. Farley, A. R. Basu, H. Craig, *Contrib. Mineral. Petrol.* **115**, 75 (1993); M. D. Kurz, P. S. Meyer, H. Sigurdsson, *Earth Planet. Sci. Lett.* **74**, 291 (1985); T. W. Trull *et al.*, *Eos* **71**, 657 (1990).
30. G. A. Macdonald and T. Katsura, *J. Petrol.* **5**, 82 (1964).

31. We thank R. Greene and L. Evans for technical assistance; C. Sinton for help with sample selection; R. A. Duncan for providing the Floreana and Santa Fe samples; W. M. White for a preprint and sharing unpublished data; S. R. Hart, C. W. Sinton, B. B. Hanan, R. A. Duncan, W. M. White, W. W. Chadwick, D. G. Pyle, and F. J. Spera for helpful discussions; and K. Farley and M. Kurz for their constructive reviews. Supported by National Science Foundation grants OCE 89-11826, 92-16913, and 92-03309.

30 July 1993; accepted 8 November 1993